

PAPER • OPEN ACCESS

The preparation of gradient titanium alloy through laser deposition

To cite this article: N Liu *et al* 2022 *IOP Conf. Ser.: Mater. Sci. Eng.* **1270** 012118

View the [article online](#) for updates and enhancements.

You may also like

- [Microstructures of Al–Al₃Ti functionally graded materials fabricated by centrifugal solid-particle method and centrifugal in situ method](#)
Yoshimi Watanabe, Qi Zhou, Hisashi Sato et al.
- [Aluminum matrix texture in Al–Al₃Ti functionally graded materials analyzed by electron back-scattering diffraction](#)
Yoshimi Watanabe, Paulo D. Sequeira, Hisashi Sato et al.
- [Surface effect on vibration characteristics of bi-directional functionally graded nanobeam using Eringen's nonlocal theory](#)
Chinika Dangi and Roshan Lal



ECS
The
Electrochemical
Society
Advancing solid state &
electrochemical science & technology

DISCOVER
how sustainability
intersects with
electrochemistry & solid
state science research

The preparation of gradient titanium alloy through laser deposition

N Liu^{1,2}, Y L Liu^{1,2}, Z L Zhao^{1,*}, H O Yang^{1,2} and W X Xu¹

¹ School of Materials Science and Engineering, Northwestern Polytechnical University, Xi'an 710072, P.R. China

² State Key Laboratory of Solidification Processing, Northwestern Polytechnical University, Xi'an 710072, P.R. China

* Corresponding author, E-mail address: zlzhao@nwpu.edu.cn

Abstract: Functionally gradient materials (FGMs) with continuous variation in composition or microstructure can realize gradient properties in different positions of the same component. The layer-by-layer laser deposition additive manufacturing is one of the most promising technologies that prepare FGMs with gradient properties. The present study is focused on the preparation of gradient titanium alloy by laser depositing Ti₂AlNb powders on the substrate of a near- α high temperature titanium alloy. The microstructure, composition, and micro-hardness of prepared gradient titanium alloy with and without transition layer were compared and analyzed. Results show that an obvious bonding interface with variant microstructure morphology and element contents formed during directly deposited Ti₂AlNb powders on near- α titanium alloy substrate and the bonding interface exhibits higher micro-hardness than the substrate and the deposited zone. However, the microstructure and the element exhibit gradient distribution characteristics along the deposition direction after adding the mixed powders of both two alloys as intermediate transition layers between the near- α titanium alloy and the Ti₂AlNb alloy. The gradient distributed micro-hardness from the substrate to the top deposited zone sufficiently demonstrates the feasibility of obtaining gradient properties of gradient titanium alloy with composition transition layer during laser depositing.

1. Introduction

Titanium alloys, which are well-known to have the characteristics of high specific strength, excellent corrosion resistance and heat resistance, play an important role in preparing many key components of the aerospace field over the past decades [1,2]. The present high-temperature titanium alloy can effectively ensure the serving temperature of components up to 600 °C for a long time. Titanium-aluminum-base alloy performs attractive high-temperature antioxidant ability, and the working temperature can reach 700-900 °C. However, the rapid development of high-performance aerospace equipment further aggravates the temperature gradients and stress gradients in different positions for some key components, which exceeds the specific serving range of traditional single composition or microstructure titanium alloys and titanium-aluminum-base alloys. Functionally graded materials (FGMs) are materials that achieve gradient properties through gradual changes in composition or microstructure [3], which is beneficial to withstand large temperature gradients and stress gradients. If the near- α high-temperature titanium alloy and the titanium-aluminum-base alloy are combined to prepare a gradient titanium alloy, the performance advantages of near- α high-temperature and titanium-aluminum-base alloy at different temperatures can both be fully utilized to realize the temperature gradient distribution required in different positions for the key component.



Recently, gradient titanium alloys can be manufactured directly through layer-by-layer laser deposition additive manufacturing [4]. The chemical composition can be changed accordingly over a large length scale by varying the pre-alloyed mixed powders during the laser deposition process, and the microstructure and properties can be controlled to obtain the gradient properties in different positions of the components. Xu et al. [5] prepared TC11/ γ -TiAl bi-materials without cracks by laser powder deposition, and found that the fracture position was located at the TiAl side rather than interfaces, and the composition and microstructure change discontinuously at the interface. Wu et al. [6] prepared γ -TiAl/Ti₂AlNb dual alloy without cracks by direct metal deposition, and discovered that a transition zone with gradual change of compositions and microstructures was generated between γ -TiAl and Ti₂AlNb alloy and an obvious boundary was observed between layers of the transition zone. Tan et al. [7] fabricated TA15/Ti₂AlNb dual alloy by laser solid forming, and found that the compositional variation tends to be continuous and smooth while the micro-hardness exhibits discontinuous characteristics. Thus, directly connecting two metals by laser deposition may result in discontinuous properties due to differences in composition and thermophysical properties.

The discontinuous properties can be effectively alleviated by adding the transition layers with a certain composition gradient between the two alloys. Ma et al. [8] fabricated TC4/TiAl bimetallic structure by laser deposition melting and found that cracks occurred in the fusion zone of TC4 and TiAl alloys. The subsequent addition of compositional transition layers composed of the two mixed powders effectively eliminated the cracks and the fabricated TC4/TiAl graded material showed a quasi-cleavage fracture with the ultimate tensile strength of 308 MPa and an elongation of 1.8%. Liu et al. [9] prepared a continuously compositionally graded Ti/Ti6Al4V material without cracks by laser powder deposition, and found that the hardness and elastic modulus gradually increase from the Ti substrate to Ti6Al4V. He et al. [10] prepared TC4/TC11 alloy specimens with different composition gradients in the transition zone by laser deposition, and found that the transition layer number has a great influence on the microstructure. The increase of the transition layer in number reduces the interface difference between TC4 and TC11 alloys, causing more uniform micro-hardness distribution and higher tensile strength and plasticity.

Most of the literature mentioned above has paid attention to the fabrication of TC4/titanium-aluminum-base alloy FGMs, while the research on the preparation of gradient titanium alloys by combining near- α high-temperature titanium alloys and titanium-aluminum-based alloys is less reported. In the present study, gradient titanium alloys with and without composition transition layer were produced by laser depositing Ti₂AlNb powders on a forged near- α high-temperature titanium alloy plate. The near- α titanium alloy and Ti₂AlNb powders with a mass ratio of 50% were used as the intermediate layer to alleviate the bonding interface between the substrate and the deposition zone. The microstructure, composition and micro-hardness of two sets of gradient titanium alloy were compared and analyzed. This study provides a theoretical and experimental foundation for manufacturing gradient titanium alloy with gradient properties through laser deposition.

2. Materials and methods

2.1. Materials

The forged near- α high-temperature titanium alloy plate (Ti-5.8Al-4.8Sn-2Zr-1Mo-0.35Si-0.85Nd) was selected as the substrate, and was milled to be flat and cleaned with alcohol for subsequent laser deposition. The microstructure of near- α titanium alloy substrate (figure 1) shows the bimodal structure which consists of equiaxed α phase and transformed β matrix, and finely α platelets are homogeneously distributed in β matrix. The diameter range and the volume fraction of primary α phases with spherical or ellipsoidal shapes are 20-40 μm and about 75%, respectively.

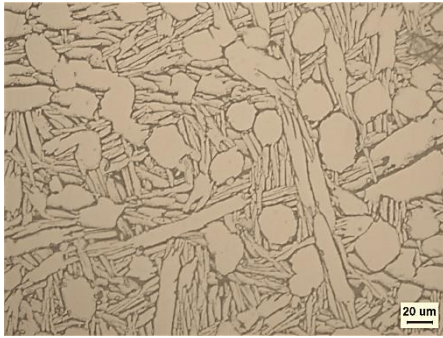


Figure 1. The microstructure of forged near- α titanium alloy substrate.

The near- α titanium alloy powder with the same composition as the substrate and Ti_2AlNb (Ti-22Al-25Nb) powder are used as raw materials for laser deposition process. The chemical composition of two raw powders is given in table 1. SEM images of the powders are shown in figure 2. The spherical powders of near- α titanium alloy and Ti_2AlNb alloy are in the size range of 74-178 μm and 53-150 μm , respectively. Before the laser deposition process, the near- α titanium alloy powder and Ti_2AlNb powder were accurately weighed with a mass ratio of 50% and mixed on a planetary ball mill for 2 h (forward rotation for 5 min, reverse rotation for 5 min, and the cycle was repeated). The mixed powders and Ti_2AlNb powders were dried by heating up to 120 ± 10 $^\circ\text{C}$ for 2 h for use.

Table 1. Chemical composition of the raw near- α titanium alloy and Ti_2AlNb powders (wt.%).

Chemical composition	Al	Sn	Zr	Mo	Si	Ta	Nb	O	Ti
Ti_2AlNb powder	10.44	0.9	-	-	-	-	43.33	0.06	Bal.
Near- α titanium alloy powder	6.14	3.68	3.43	0.52	0.55	0.96	0.40	0.12	Bal.

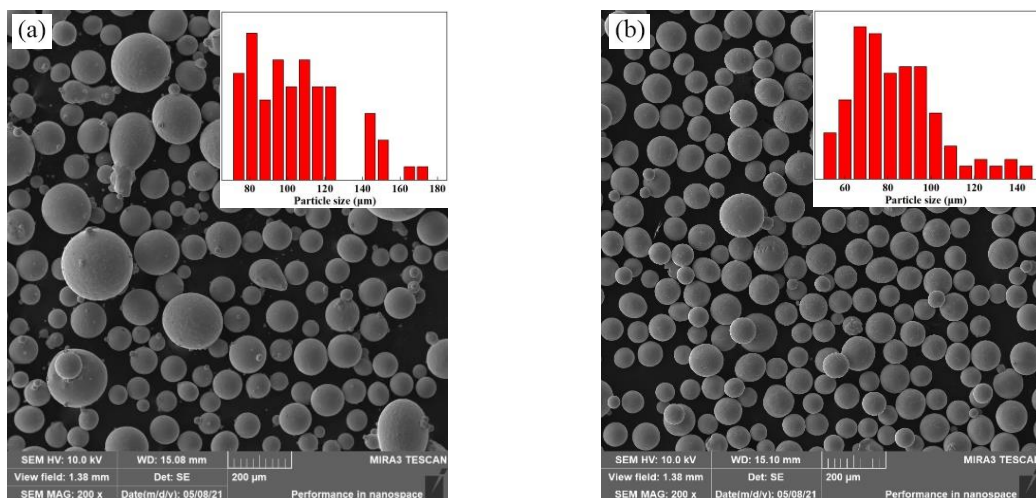


Figure 2. SEM images of raw powders: (a) near- α titanium alloy and (b) Ti_2AlNb alloy.

2.2. Sample preparation

The laser deposition process was conducted in an LSF-VI machine equipped with a maximum 6 kW semiconductor laser, a high-precision powder feeder, a five-axis four linkage CNC worktable and a coaxial powder feeder with four nozzle tips. The process was conducted under a constant flow of ultra-high purity Ar to minimize the oxygen contamination (residual oxygen concentration, under 50 ppm). The substrate was fixed on the horizontal workbench (along x-y direction), and the alloy powders were fed into the molten pool produced by a laser beam, then the molten metal powder solidified on the substrate, and then deposition layers were formed with the stepped movement of a laser beam and powder feed head in the z-direction, the schematic diagram is shown in figure 3.

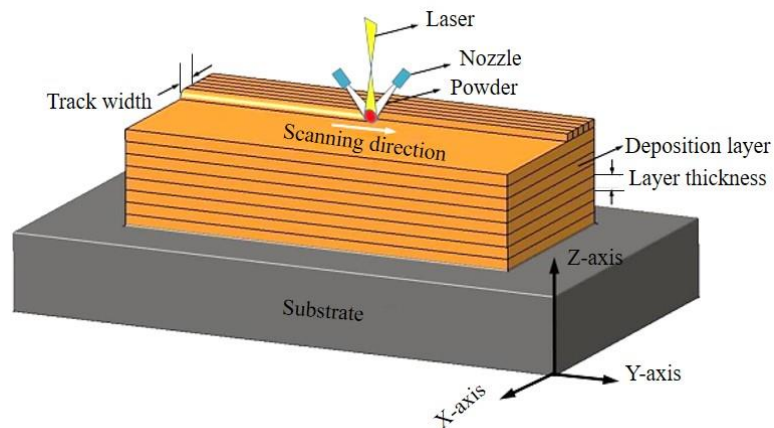


Figure 3. Schematic diagram of the working principle of laser deposition.

Two sets of laser deposition experiments were designed in this study, the planned composition of samples is given in figure 4. The process parameters used for the deposition of the two sets of samples are basically consistent, including the scanning rate of 1000 mm/min, the beam diameter of 3 mm, and the increment of the Z-axis of 0.3 mm. The laser powers of 2.2-2.8 kW were used in laser depositing Ti_2AlNb powders on the near- α titanium alloy substrate, and the laser power of 2.8 kW was used in the preparation of gradient titanium with a composition transition layer. The scanning was bi-directional and the scanning direction was kept 90° between the two successive layers.

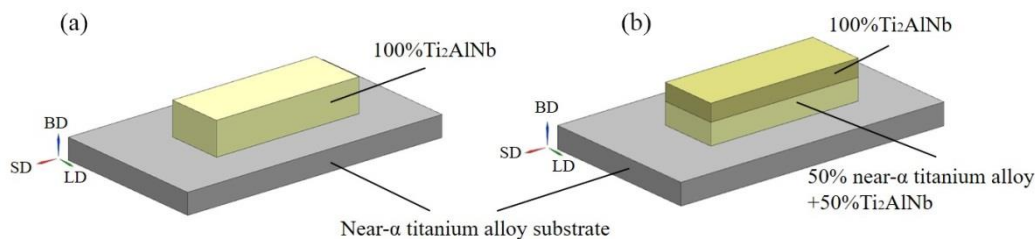


Figure 4. Schematic of samples with the planned composition (SD implies scanning direction; LD implies lateral direction; BD implies building direction).

2.3. Sample characterization

The as-fabricated samples were wire-cut in the longitudinal direction and metallographically prepared to observe the variation in the microstructure, elemental composition and micro-hardness from the forged substrate to deposition layers. The samples were etched using Kroll's reagent (2 vol% HF, 3 vol% H_2O_2 and 7 vol% HNO_3 in 20 vol% water) for 30 s. The microstructural observation was carried out with an optical microscope (OM, OLYMPUS GX-71). The elemental distribution was conducted by a scanning electron microscope (SEM, G3 UC) equipped with energy dispersive spectroscopy (EDS). The Vickers micro-hardness was measured with a regular spacing of 0.3 mm by a digital micro-hardness tester (LECO) at a load of 200g and an indentation time of 13s.

3. Results

3.1. The microstructure of laser depositing Ti_2AlNb powders on the near- α titanium alloy substrate

Optical micrographs of laser depositing Ti_2AlNb powders on the near- α titanium alloy substrate are illustrated in figure 5. It could be found that the deposited Ti_2AlNb alloy is free of cracks and well-bonded with forged near- α titanium alloy substrate, and a dense and bright bonding interface with a certain width is formed between the two alloys. The microstructures on both sides of the bonding

interface are of comparatively large discrepancy. In the heat-affected zone (HAZ) of the near- α titanium alloy substrate near the interface (5(a)), the lamellar α and equiaxed α phase gradually decrease and disappears and the coarsen equiaxed β grain boundaries are visible. The equiaxed grains in the HAZ gradually transform into columnar grains in the first few deposition layers due to the directional solidification and epitaxial growth [11].

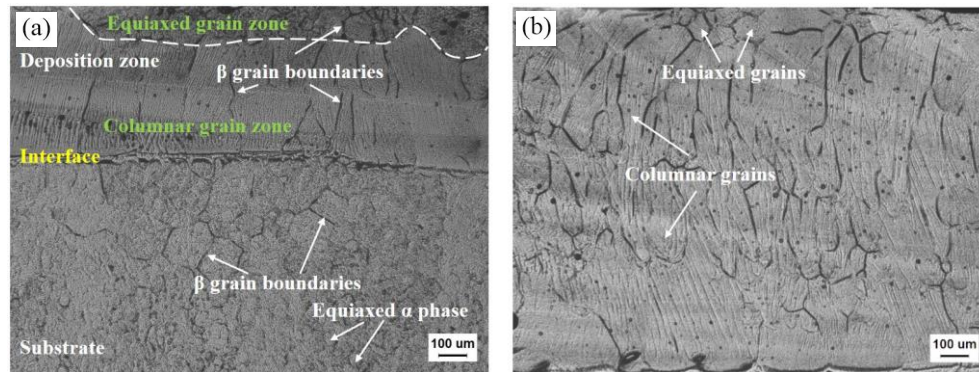


Figure 5. Optical micrographs of laser depositing Ti_2AlNb powders on the near- α titanium alloy substrate with the laser power of 2.8 kW: (a) the microstructure surrounding the bonding interface and (b) deposited Ti_2AlNb zone.

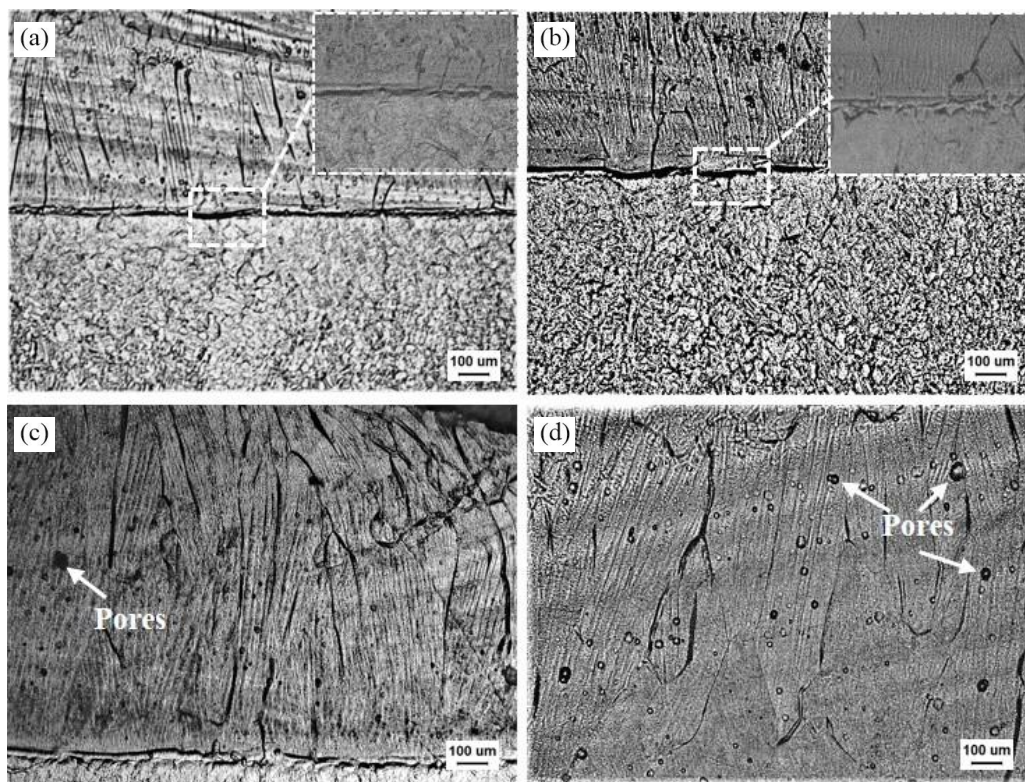


Figure 6. Microstructure of laser depositing Ti_2AlNb powders on the near- α titanium alloy substrate under different laser powers: the bonding interface under (a) 2.2 kW, (b) 2.5 kW; deposited Ti_2AlNb zone under (c) 2.2 kW and (d) 2.5 kW.

The microstructure of laser depositing Ti_2AlNb powders on the near- α titanium alloy substrate under different laser powers is shown in figure 6. It can be seen from these figures that under a large laser power input the clearer bonding interface with no defects will be formed, and the width of β grains at the Ti_2AlNb deposition zone will increase, while the length of β grains increase under a small laser

power input. The different laser powers used in the laser deposition process have no influence on the microstructure constitution. There exist pores within the deposited Ti_2AlNb zone under the laser power of 2.2 kW and 2.5 kW, whose size is about 10 μm . Compared to 2.8 kW (figure 5(a)), it can be found that a large laser power input is beneficial to reduce this kind of metallurgy defect.

3.2. The gradient microstructure of gradient titanium alloy with the composition transition layer

In order to attenuate the microstructure mutation at the bonding interface of the near- α titanium alloy substrate and the Ti_2AlNb deposition zone, a composition transition layer composed of 50% near- α titanium alloy and 50% Ti_2AlNb mixed powders was added between the two alloys. The overall macrostructure morphology of the gradient titanium alloy with composition transition layer and the microstructure of different composition zones were displayed in figure 7. It can be discovered that good metallurgical bonding was obtained between the different composition zones of the gradient titanium alloy, and no defects are observed. The grain morphology of different regions can be clearly observed, as shown in figure 7(b)-7(e).

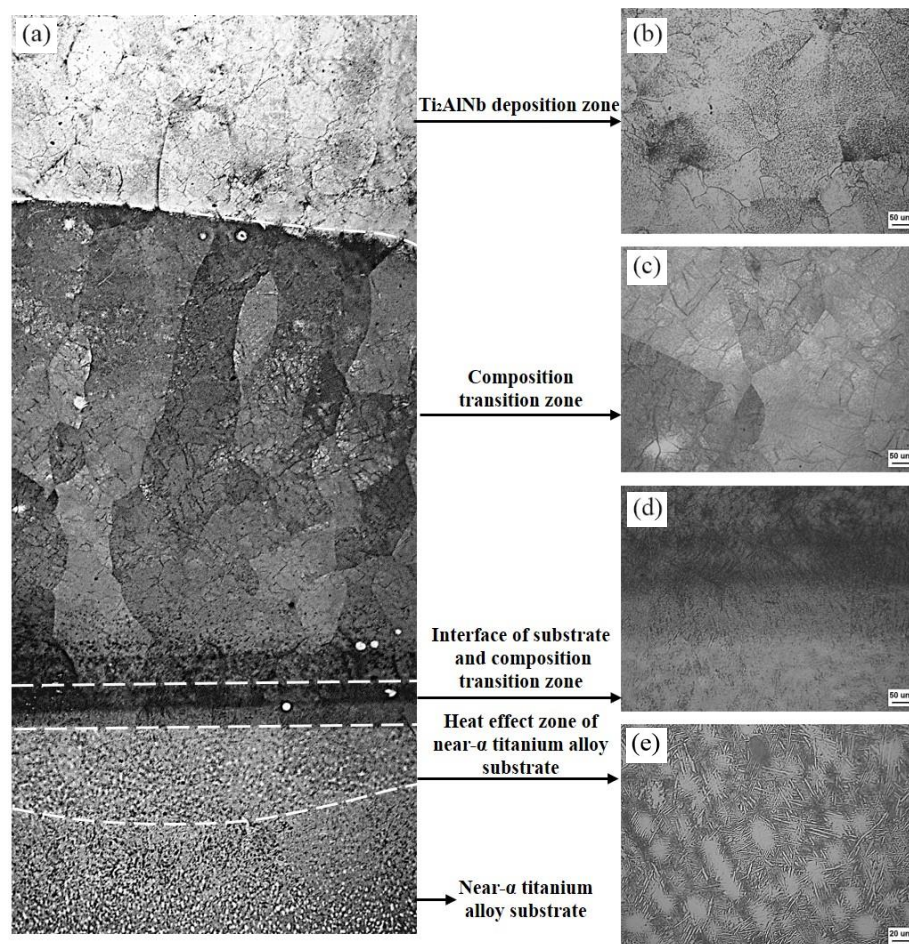


Figure 7. Macrostructure of the gradient titanium alloy with composition transition layer: (a) the overall view; (b) Ti_2AlNb deposition zone; (c) composition transition zone; (c) interface of substrate and composition transition zone; (d) HAZ of substrate and (e) near- α titanium alloy substrate.

The interface of the α/β phase in HAZ is fuzzy in comparison with the duplex structure of the forging. The gradual disappearance of equiaxed α grains and the precipitation of secondary lath α clusters from the β matrix (figure 7(e)) are related to the complex thermal history experienced by the near- α titanium alloy substrate during the rapid solidification of the deposited layer, which is characterized by its cyclic reheating and high cooling rates [15,16]. The smooth interface with a certain width between the

composition transition zone and the near- α titanium alloy substrate was observed, as shown in figure 7(d). The formation of the interface has a great relationship with the change of alloy composition.

The microstructure of the composition transition zone (figure 7(c)) is mainly composed of coarse columnar crystals that penetrate through multiple deposition layers and grow epitaxially. The length of the β grains is within 300–1500 μm , averaging approximately 300 μm in width. The direction of the columnar crystals is parallel to the deposition direction, and there are river-shaped sub-grain boundaries inside the grains. The generation of the sub-grain boundaries may be related to the rapid solidification process during laser deposition. Additionally, no interface was formed between 50% near- α titanium alloy+50% Ti_2AlNb deposition layers and the Ti_2AlNb deposition zone due to the similar chemical composition.

The microstructure of the Ti_2AlNb deposition zone (figure 7(b)) is comprised of equiaxed coarse grains that had an average diameter of approximately 200 μm , which is due to the tendency to obtain equiaxed grains of the alloy during the laser deposition process can be significantly improved by the introduction of elements such as Nb. The result was confirmed in previous research. Zhang et al. [17] obtained a fully equiaxed grain microstructure during the laser solid formed TC21 titanium alloy (Ti-6Al-2Sn-2Zr-3Mo-1.5Cr-2Nb) by increasing the powder feeding amount, and it is considered that appropriate alloying elements such as Mo, Cr, B are crucial to obtain equiaxed β grains in laser solid formed titanium alloys, rather alloying elements such as Al, Sn, and Zr have little effect on CET behavior. In general, the graded microstructure that transforms from duplex to columnar and then to equiaxed coarse grains along the deposition direction was formed.

3.3. The composition differences of gradient titanium alloy with and without composition transition layer

The distribution of elements across the bonding interface of near- α titanium alloy and Ti_2AlNb alloy is shown in figure 8, an obvious change in the element content of Ti, Nb, and Al on the sides of the bonding interface is observed. Among them, the content of the Ti element decreases from 85% to about 70%, while the content of the Nb element increases from 10% to about 25%. Accordingly, the content of the Al element is stepwise increased but it is not obvious. The content of the Sn element has almost no fluctuation. The variation of composition distribution can be explained by the characteristic of the laser deposition process. Once deposition starts, part of the substrate is melted and mixed with new-deposited Ti_2AlNb alloy to form a layer with composition between them. As deposition continues, the composition of the newly developed layer is closer to Ti_2AlNb alloy. At last, the interface with changed compositions is established between the substrate and the Ti_2AlNb deposition zone.

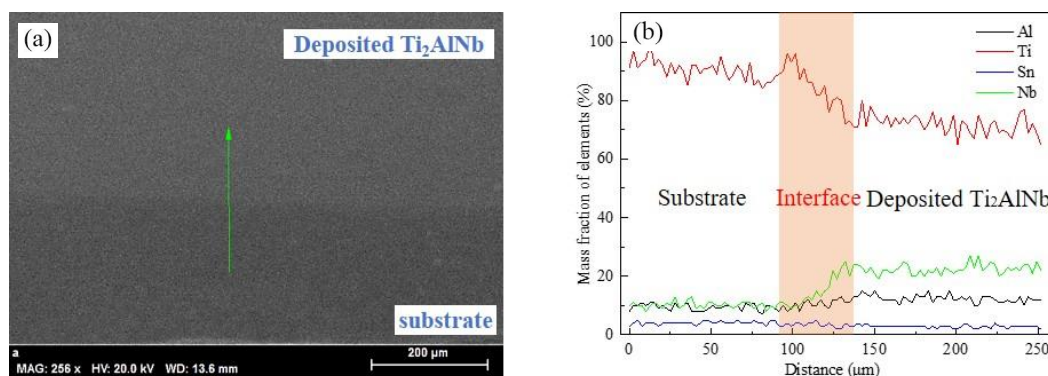


Figure 8. Composition variation across the interface of near- α titanium alloy and Ti_2AlNb alloy: (a) scanning direction and area and (b) EDS curve.

In general, the elements' content of the bonding interface is different from that of the two alloys, which demonstrates the microstructure morphology is also different. As consequence, it indicates that a certain degree of microstructural and compositional abrupt change between the two alloys occurred at the bonding interface during the laser deposition process, which may affect the performance

continuity during the laser depositing Ti_2AlNb powders on the near- α titanium alloy substrate. The composition transition layer added between the two alloys improves the compositional continuity, and the composition distribution of the gradient titanium alloy with composition transition layer was displayed in figure 9. It can be noticed that the content of the main alloy elements, Ti, Al and Nb, are distributed continuously and showed a nearly linear change as a result of sufficient diffusion between the layers [18]. The element of Sn is stepwise decreased, but not obvious because of the low content, which was also found in previous studies about TA15 (near- α titanium alloy)- Ti_2AlNb FGMs by Chen et al. [19,20]. Overall, the smooth gradual change exhibited in the gradient titanium alloy with composition transition layer is preferred to directly deposit Ti_2AlNb powders on the near- α titanium alloy substrate, because the gradient change can decrease the discontinuity of its microstructures and properties. As consequence, the feasibility of preparing gradient titanium alloy with gradient composition by laser deposition is confirmed.

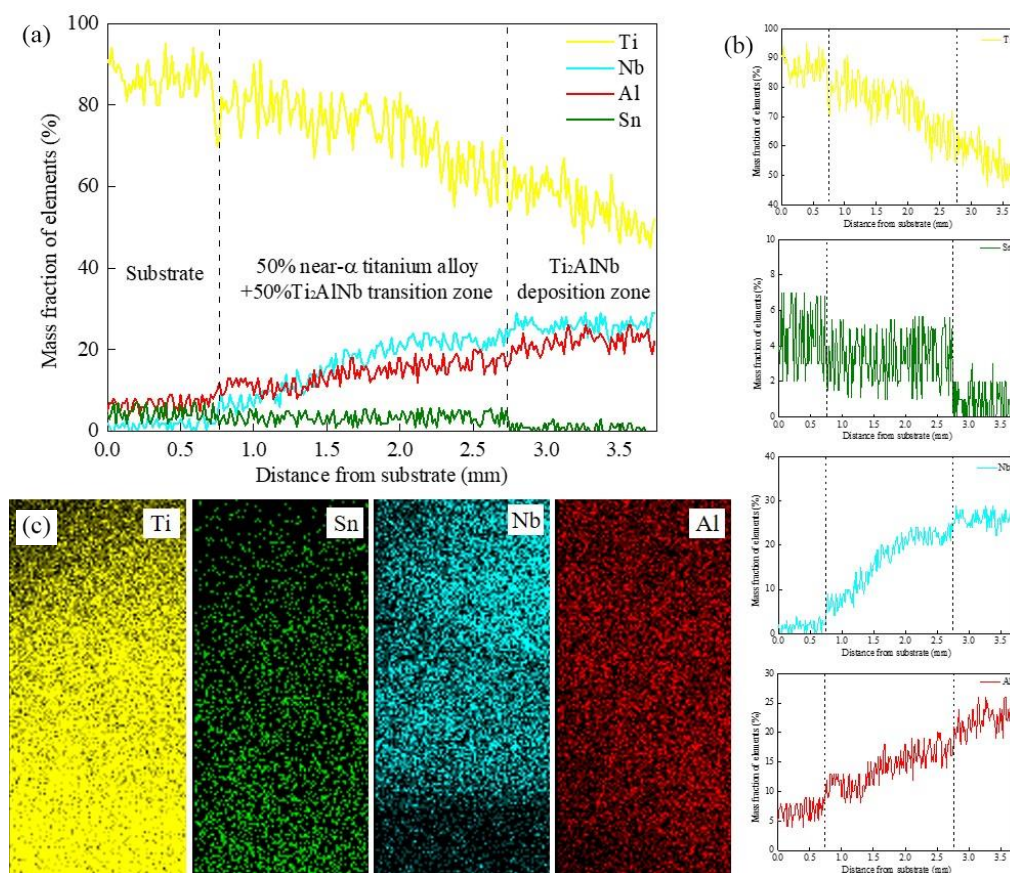


Figure 9. Composition distribution of gradient titanium alloy with composition transition layer: (a) EDS line scanning results of main alloy elements; (b) variation trend of the content of each element in figure 9(a); (c) face scanning results.

The thermal behavior of the deposition process is a special cyclic thermal process; that is, previous deposited layers will be strongly heat-affected by subsequently deposited layers. Under the continuous influence of the laser heat source, elements diffusion occurs, and the element concentration C_x at a depth x after a certain time t can be roughly estimated according to Fick's second law.

$$\frac{C_x - C_0}{C_s - C_0} = 1 - \operatorname{erf}\left(\frac{x}{2\sqrt{Dt}}\right) \quad (1)$$

Where C_0 refers to the element concentration at distance x before diffusion, the C_s refers to the concentration of an alloying element in the molten pool, and D refers to the diffusion coefficient of

the element. It can be inferred that the element concentration is mainly related to the diffusion time and diffusion coefficient, and it is easy for a high diffusion coefficient to realize uniform diffusion behavior at the same diffusion time. Gu [21] found that the diffusion coefficient of Ti is larger than Nb and Al in the Ti-Al-Nb (body-centered cube) alloys. Therefore, Ti element has a smoother transition than Al and Nb elements.

3.4. Micro-hardness distribution differences of gradient titanium alloy with and without composition transition layer

Figure 10 shows the micro-hardness distribution of the two sets of gradient titanium alloy samples. The micro-hardness at the newly formed bonding interface is higher than the substrate and deposited zone during laser deposit Ti_2AlNb powders on the near- α titanium alloy substrate under different laser power conditions, as illustrated in figure 10(a). The precipitation of the martensite α' phase with fine acicular Widmanstätten morphology should be responsible for the higher micro-hardness value at the bonding interface. The micro-hardness of the near- α titanium alloy substrate is about 329 HV and gradually increases along the deposition direction until reaches a peak at the bonding interface. Subsequently, the micro-hardness decreases to about 384 HV, then gradually rises to 496 HV and finally remains stable.

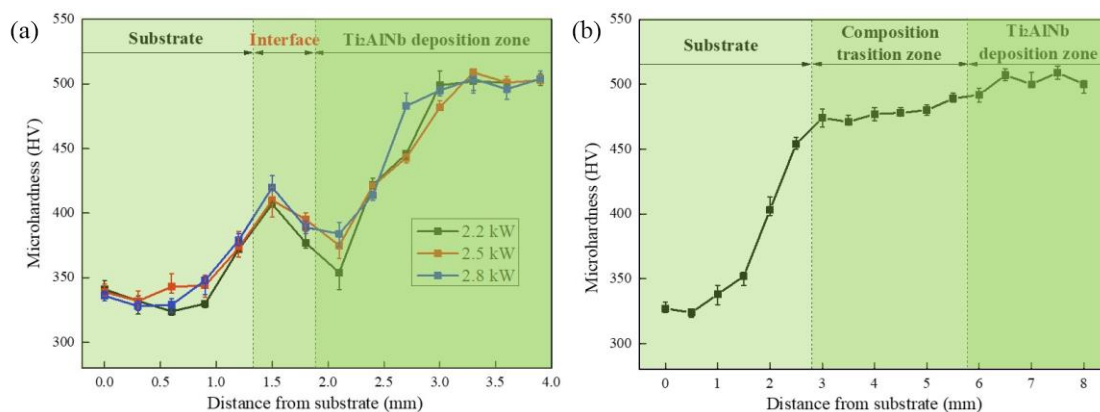


Figure 10. Micro-hardness distribution: (a) laser depositing Ti_2AlNb powders on the near- α titanium alloy substrate under different laser powers and (b) the gradient titanium alloy with composition transition layer at the laser power of 2.8 kW.

The variation trend of the micro-hardness obtained under different laser powers is consistent from near- α titanium alloy substrate to the Ti_2AlNb powder deposition zone, especially the micro-hardness values at the bonding interface are basically the same. When the laser power increased from 2.2 kW to 2.8 kW, the micro-hardness at the bonding interface changed from 405 HV to 420 HV, and the difference was not particularly obvious. Besides, it can be seen from figure 10(a) that higher laser power can reduce the micro-hardness differences of the material along the deposition direction, making the overall properties of the material relatively more uniform, which may be attributed to the diffusion of Al and Nb elements more sufficient at higher powers.

The micro-hardness values of the near- α titanium alloy substrate, the composition transition zone, and the Ti_2AlNb deposition zone are different, as shown in figure 9(b). The average micro-hardness of the substrate is about 334 HV, then a rapid increase appears at HAZ. The rapid increase of HAZ is not only inseparable from fine basketweave structure induced by the large temperature gradient, but also related to the precipitation of brittle α_2 phase resulting from the diffusion of Al element from the composition transition zone, and the diffusion of Nb element also exacerbates the solid solution strengthening effect. The micro-hardness in 50% near- α titanium alloy+50% Ti_2AlNb composition transition zone is about 460-480 HV, showing a slow upward trend along the deposition direction.

The micro-hardness of the interface of the composition transition zone and Ti₂AlNb deposition zone changes continuously and steadily, which is attributed to the composition on both sides of the interface being more similar. As a result, the degree of microstructural change decreases, and a good gradient transition between the composition transition zone and Ti₂AlNb deposition zone can be obtained. A little micro-hardness fluctuation is observed at the Ti₂AlNb deposition zone, and the micro-hardness is stable at approximately 500 HV. Taking into consideration, the continuous increase of micro-hardness along deposition direction can be basically realized at the composition ratio of 50% near- α titanium alloy+50% Ti₂AlNb, which demonstrates the feasibility of preparing gradient titanium alloy with gradient properties by laser deposition technology.

4. Discussion

According to the above results and analysis, the microstructure evolution of gradient titanium alloy with and without composition transition layer is elucidated. It's known that the deposited layers experienced several thermal cycles during the laser deposition process, and the microstructures of titanium alloy were changed due to the phase transformation of the solid [22].

For the titanium alloy of laser depositing Ti₂AlNb powders on the near- α titanium alloy substrate, the HAZ is thermally affected by the laser and rapidly cooled, and the α' martensite phase is formed in the region. The closer to the bonding interface, the finer the phase, the more α/β phase interface, and the increase in micro-hardness, which is consistent with figure 10(a). According to the EDS result (figure 8), the content of α -stabilizing element Al at the bonding interface near the deposition zone is low, only about 11%, while the content of β -stabilizing element Nb is relatively high, which restricted the formation of α or α_2 phase, so the obtained phase structure is mainly $\beta/B2$ phase. With the increase of the deposition layer, the Nb content gradually increased to 22%, and the Al content also increased to 14%, so the hard brittle α_2 and orthorhombic O phase formed, and the phase constitution changed from $\beta/B2$ to $\alpha_2+\beta/B2+O$ phase.

During the LSF process, the metal powder is melted and solidified layer by layer through laser heating to achieve a 3D shape, so when a new deposition layer is formed, the alloy that has been formed at the bottom of the molten pool will be thermally affected, which can be considered as the aging treatment of the deposited metal [23]. With the increase of Nb content, the phase region moves to the (α_2+B2+O) region, where aging will produce the dendritic O phase distributed in the B2 matrix. The reason for the appearance of the O phase may be the transformation of the α_2 phase, B2 phase, or the clathrate reaction of α_2+B2 [24]. Since the content of the α_2 phase is relatively low when the deposition height is low, according to the analysis, it is believed that the formation of the O phase is mainly due to the shearing of the B2 phase to form transition phase B19, and then B19 is further ordered to form O phase. The main phase in the equiaxed grain region is the dendritic O phase with different thicknesses distributed in the $\beta/B2$ matrix, and a small amount of α_2 exists in the equiaxed prior β grain boundary.

5. Conclusions

- An obvious bonding interface with variant microstructure morphology formed during directly depositing Ti₂AlNb powders on the near- α titanium alloy substrate. The microstructure in the HAZ of the substrate side exhibited coarse grains, rather the deposition zone side showed typical columnar grains, and the large laser power increases the width of β grains.
- The graded microstructure that transforms from duplex to columnar and then to equiaxed coarse grains along the deposition direction was formed at the gradient titanium alloy by adding two mixed powders of two alloys as intermediate transition layers between near- α titanium alloy and Ti₂AlNb alloy.
- On the sides of the bonding interface, the element content of Ti, Nb, and Al changed obviously from the near- α titanium alloy substrate to the deposited Ti₂AlNb zone. The element exhibited a gradient distribution along deposition direction at the gradient titanium alloy with intermediate transition layers.
- The bonding interface exhibits higher micro-hardness than the substrate and the deposited zone

indicated the discontinuous change characteristics of directly depositing Ti₂AlNb powders on the near- α titanium alloy substrate. Inversely, the gradient distributed of micro-hardness from the substrate to the top deposited zone can be basically realized after adding 50% near- α titanium alloy+50% Ti₂AlNb composition transition zone.

References

- [1] Narayana P L, Kima S W, Honga J K, Reddyb N S and Yeoma J T 2018 *Mater. Sci. Eng.* **718** 287-91
- [2] Lu J Z, Lu H F, Xu X, Yao J H, Cai J and Luo K Y 2020 *Int. J. Mach. Tool Manufact.* **148** 103475
- [3] Zhang C, Chen F, Huang Z, Jia M, Chen G, Ye Y, Lin Y, Liu W, Chen B, Shen Q, Zhang L and Enrique J L 2019 *Mater. Sci. Eng. A* **764** 138209
- [4] Qi Z L, Chen J, Zhou Q J, Yan Z Y and Huang W D 2020 *Appl. laser* **40** 214-20
- [5] Xu Z J, Zhang Y Z, Liu M K and Gong X Y 2016 *Rare Met.* **35** 456-62
- [6] Wu Y, Cheng X, Zhang S, Liu D and Wang H 2019 *Intermetallics* **106** 26-35
- [7] Tan H, Mi Z, Zhu Y, Yan Z, Hou X and Chen J 2020 *Mater.* **13** 552
- [8] Ma R, Liu Z, Wang W, Xu G and Wang W 2020 *Vac.* **177** 109349
- [9] Liu Y, Liang C, Liu W, Ma Y, Liu C and Zhang C 2018 *J. Alloys Compd.* **763** 376-83
- [10] He B, Liu J and Yang G 2019 *Rare Met. Mater. Eng.* **48** 910-5
- [11] Chi J, Cai Z, Zhang H, He D, Zhang H, Wan Z, Peng P and Guo W 2021 *Mater. Sci. Eng. A* **818** 141382
- [12] Hunt J D 1984 *Mater. Sci. Eng.* **65** 75-83
- [13] Zhang S, Zhang Q, Zheng M, Hu Y, Sui S, Chen J and Lin X 2021 *Mater. Sci. Eng. A* **800** 140388
- [14] Keshavarzkermani A, Sadowski M, Ladani L 2018 *J. Alloys Compd.* **736** 297-305
- [15] Attar H, Shima E H, Kent D, Wu X and Matthew S D 2017 *Mater. Sci. Eng. A* **705** 385-93
- [16] Liang S, Li J, Zhang Q and Chen J 2021 *J. Mater. Eng. Perform.* **30** 2967
- [17] Zhang Q, Chen J, Lin X, Tan H and Huang W D 2016 *J. Mater. Process. Technol.* **238** 202-11
- [18] Tan H, Mi Z, Zhu Y, Yan Z, Hou X and Chen J 2020 *Mater.* **13** 552
- [19] Zhou Q, Qi Z, Yan Z, Chen J and Huang W 2020 *Appl. laser* **40** 421-429 (in Chinese)
- [20] Qi Z, Chen J, Zhou Q, Yan Z and Huang W 2020 *Appl. laser* **40** 214-20 (in Chinese)
- [21] Gu Y, Fan F, Guo Y, Xu G, Hui C, Zhou L and Cui Y 2018 *Calphad* **62** 83-91
- [22] Ma J, Zhang Y, Li J, Cui D, Wang Z and Wang J 2021 *Mater. Sci. Eng. A* **811** 140984
- [23] Wang J, Luo Q, Wang H, Wu Y, Cheng X and Tang H 2020 *Addit. Manuf.* **32** 101007
- [24] Goyal K and Sardana N 2021 *Mater. Today: Proc.* **41** 951-68

Acknowledgments

This study was financially supported by the National Natural Science Foundation of China (No. 51974259) and the Xi'an Municipal Bureau of Science and Technology (No. 21ZCZZHXJS-QCY6-0008).